Volume 16, Issue 2, 162511 (1-8)

International Journal of Nano Dimension (IJND)

https://doi.org/10.57647/j.ijnd.2025.1602.11

Synthesis of new ethyl cyanoacetate analogs catalyzed by nano-Fe_3O_4@EA

Tahereh Moradhosseini[1], Masoud Mokhtary [1,*], Mohammad Nikpassand[1], Majid Kia [1], Leila Asadpour[2]

[1]*Department of Chemistry, Rasht Branch, Islamic Azad University, Rasht, Iran.*
[2]*Department of Microbiology, Rasht Branch, Islamic Azad University, Rasht, Iran.*

*Corresponding author: ma.mokhtary@iau.ac.ir

Original Research

Received:
18 July 2024
Revised:
2 November 2024
Accepted:
9 November 2024
Published online:
1 April 2025

Abstract:
In this research, we present an effective method for synthesizing new derivatives of ethyl cyanoacetate through base-free Knoevenagel condensation using ellagic acid-bonded magnetic nanoparticles (nano-Fe_3O_4@EA) as a catalyst. This method offers several advantages, including high yield, short reaction time, and simplicity, making it an attractive and efficient option in the emerging field of Knoevenagel condensation.

Keywords: Ethyl cyanoacetate; Ellagic acid; Formylarylsulfonates; Knoevenagel condensation; Magnetic nanoparticles

1. Introduction

Ethyl 2-cyano-3-phenyl acrylates are considered important organic compounds with various applications in pharmaceutical and chemical industries. The synthesis of these compounds through the Novenagle reaction is an efficient and common method for their production. The unique properties of these compounds make them valuable intermediates in the synthesis of more complex compounds and active substances in various industries [1–3]. Tyrphostins are tyrosine phosphorylation inhibitors that can inhibit the catalytic activity of epidermal growth factor (EGF) receptors. One of these compounds, cyanothiocinamide, not only has anti-proliferative properties on human keratinocytes but also inhibits EGF receptor autophosphorylation (figure 1) [4].

Some derivatives of ethyl 2-cyano-3-phenyl acrylates have shown potential as anti-cancer agents. These compounds may work through various mechanisms, such as inducing apoptosis, inhibiting cell proliferation, and interfering with cell signaling pathways that support the growth and survival of cancer cells. Similarly, some derivatives of methyl 2-cyanoacrylates and methyl 2-cyano-3-phenyl acrylates have the potential for bacterial mutagenesis. These findings could serve as a basis for additional research on the safety and environmental impact of these compounds [5]. Additionally, some derivatives of ethyl 2-cyano-3-phenyl acrylates exhibit significant antimicrobial properties. These compounds can be used as antibacterial and antifungal agents to treating microbial infections. The mechanism of action often involves disrupting the cell wall of microbes or inhibiting essential enzymes for their survival [6].

2-Cyano-3-phenyl acrylates have been used in photosensitive compounds due to the distinctive properties of alpha-cyano and nitro groups. The presence of these groups in the molecule's structure can lead to unique optical properties, making it ideal for applications like light-sensitive materials (photoresists), photochromics, and other materials utilized in the electronics and optoelectronic industry [7]. Due to their chemical structure, 2-cyano-3-phenyl acrylates can serve as an intermediate in the synthesis of various compounds, including plant growth regulators. Plant growth

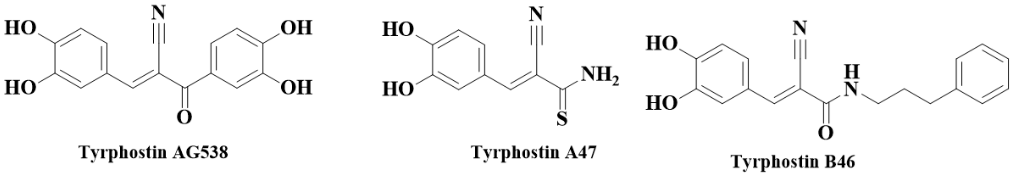

Figure 1. Some tyrphostin compounds with inhibitory properties.

regulators are substances used in small amounts to regulate or modify physiological processes in plants and can have multiple effects on plant growth and development [8]. 2-Cyano-3-phenyl acrylates with alkoxy or hydroxyl substitution are employed as ultraviolet (UV) filters due to their chemical and optical properties. These compounds can effectively absorb ultraviolet light and protect photosensitive materials from photodegradation [9]. In 2015, Schneider and his colleagues reported the Novnagel condensation for the first time using copper as a catalyst with high activity and excellent efficiency. Inexpensive and readily available copper powder was utilized to catalyze the condensation of cyanoacetate and benzaldehyde under mild conditions [10]. In 2012, a report utilized L-proline as an environmentally friendly catalyst for the Knoevenagel condensation reaction between indole-3-carboxaldehydes, N-methyl derivatives, and ethyl cyanoacetate as an active methylene combination [11]. In 1994, Kada and his colleagues successfully synthesized ethyl 2-cyano-3-furyl)acrylate by reacting formaldehyde with ethyl cyanoacetate in the presence of sodium ethoxide [12]. In 2020, Xu and his colleagues achieved the Knoevenagel condensation between benzaldehyde and ethyl cyanoacetate using three polyoxomolybdates with new organophosphonate functional groups that they synthesized [13]. Almeida and Cardoso investigated the reaction between n-butyraldehyde and ethyl cyanoacetate using Y zeolite containing trimethyl-, tetramethyl-, propyl-, and butylammonium cations [14]. The catalytic activity of a magnetic cored amino group terminated dendrimer ($Fe_3O_4@SiO_2@PAMAM\text{-}G_2$) and ionic liquid–triethanolammonium bicarbonate ([$Fe_3O_4@Si\text{-}(CH_2)_3\text{-}TEA$][HCO_3]) were studied for the Knoevenagel condensation reaction of aldehydes with malononitrile under mild and solvent-free conditions [15, 16]. Furthermore, the study investigated the use of potassium natural asphalt sulfonate (K-NAS) and UiO-66@schiff-base-Cu(II) metal-organic framework as recyclable solid nanocatalysts in Knoevenagel condensations [17, 18]. Magnetic nanocatalysts have garnered attention for their easy manipulation, large surface area, and ability to be targeted by a magnetic field. This makes their isolation from the reaction environment remarkably simple [19–32].

2. Experiments

The chemicals used were obtained from Merck, Germany, and were used without the need for purification. To monitor the progress of the reactions, thin-layer chromatography (TLC) technique was employed using aluminum sheets coated with silica gel 60, F256. Various spectroscopic techniques were utilized to analyze the molecular structures of the products. Infrared spectrometry (FT-IR) was conducted on the samples using a Shimadzu model 8900 device. Nuclear magnetic resonance spectroscopy (NMR) was performed using 300 MHz and 75 MHz Bruker devices in DMSO-d6 solvent, with TMS serving as the internal reference. The melting temperatures of the samples were determined using a 9200 model electrothermal device. The crystalline structure of the nanocatalyst was determined by a Philips (PW1730), XRD instrument at λ = 1.54056 ^{O}A. LC-MS was performed using a Shimadzu UFLC LC-AD20 system (Japan)-3200 QTRAP mass spectrometer instrument (AB Sciex, MA, USA). The LC conditions were as follows : Mobile phase : CH_3OH + 0.1%, HCOOH : H_2O + 0.1% HCOOH 95 : 5, Column: Kromasil 100-5 C18 column (150 mm $\times$4.6 mm), column temperature: 30 ^{o}C, flow rate: 0.25 ml/min. The MASS conditions were as follows:Mode: ESI+, capillary voltage: 4.5 kV, gas nebulizer: N_2 (grade 5), desolvation temperature: 450 ^{o}C, declustering potential (DP): 10 V, ion source gas 1 : 40 psi, ion source gas 2: 50 psi.

2.1 Synthesis of nano-Fe_3O_4@EA nanoparticles

First, nano-Fe_3O_4 (1 g) were dispersed in toluene (50 mL) using an ultrasound bath for 15 minutes. Then, (3-chloropropyl) triethoxysilane (2 mL) was added to the mixture and refluxed for 1 hour. The resulting powder was separated from the filter paper and dried in an oven for 24 hours at 80 ^{o}C. To synthesize nano-Fe_3O_4@EA, ellagic acid (0.3 g) was dissolved in DMSO (30 mL). Then, nano-$Fe_3O_4@Si(CH_2)_3Cl$ (0.15 g), KI (0.17 g), and NaOH (2 mL, 0.08 M) were added to the mixture and dispersed using an ultrasound bath for 2 hours. Finally, the nano-Fe_3O_4@EA was isolated using filter paper and dried in an oven at 80 ^{o}C.

2.2 General method for the synthesis of formylarylsulfonates

In a 50 mL round bottom flask, 10 mmol of hydroxy aldehydes, 10 mmol (1.12 g) of DABCO and 10 mmol (1.90 g) of benzenesulfonylchloride or toluenesulfonylchloride in 10 mL of acetonitrile solvent were dissolved. The reaction was stirred under reflux conditions for 3 hours with a magnetic stirrer. The progress of the reaction was monitored by TLC. After the completion of the reaction, the product was extracted from the reaction mixture with CH_2Cl_2 and 10% sodium chloride, and the organic phase was dried with 0.5 g of sodium sulfate. The resulting product was crystallized in ethanol for further purification.
The melting points of known compounds were compared to those of the authentic samples reported in the literature. mp**1a**: 65-67 ^{O}C, mp**1b**: 73-74, reported: 72-73 ^{O}C [33];

mp**1c**: 63-64 ^{O}C, reported 64-65 ^{O}C [34]; mp**1d**: 54-56 ^{O}C, reported: 53-56 ^{O}C [36]; mp**1e**: 66-68 ^{O}C, reported: 64-66 ^{O}C [35]; mp**1f**: 126-129, reported: 126-128 ^{O}C [38]; mp**1g**: 104-106 ^{O}C, mp**1h**: 94-96 ^{O}C, reported: 97-98 ^{O}C [36], mp**1i**: 90-92 ^{O}C.

2.3 General method for the synthesis of 2-cyano-3-phenyl acrylate analogs

Synthetic aldehyde (1 mmol), ethyl cyanoacetate (2 mmol), and nano-Fe_3O_4@EA catalyst (0.05 g) were added to a 10 mL round bottom flask under reflux conditions with ethanol (5 mL). The progress of the reaction was monitored using thin layer chromatography (EtOAc/*n*-hexane/MeOH, 4 : 6 : 1). After the reaction was complete (2-3 hours), the mixture was cooled, filtered to remove any sediment, and the products were separated using filter paper. The structure of the product was identified using FT-IR, ^{1}H-NMR, and ^{13}C-NMR spectroscopy.

2.4 Characterization of nano-Fe_3O_4@EA

The fabrication stages of nano-Fe_3O_4@EA are shown in figure 2. The ellagic acid functionalization on the surface of nano-Fe_3O_4 was achieved using the layer-by-layer construction method. Initially, the nano-Fe_3O_4 was reacted with (3-chloropropyl) triethoxysilane to generate nano-Fe_3O_4@$Si(CH_2)_3Cl$ particles. Later, ellagic acid was added to react with the nano-Fe_3O_4@$Si(CH_2)_3Cl$. Subsequently, the nano-Fe_3O_4@EA was prepared.

The functionalization of nano-Fe_3O_4 using ellagic acid was confirmed through FT-IR analysis. The FT-IR analysis of nano-Fe_3O_4@EA showed stretching vibrations of OH at 3194 cm^{-1}, C=O at 1713 cm^{-1}, C = C at 1621 cm^{-1}, and C-O at 1025 cm^{-1}. Additionally, Fe-O stretching vibrations were find at 550 cm^{-1} (refer to figure 3). A comparison of the FT-IR spectra of ellagic acid, nano-Fe_3O_4@EA@$Si(CH_2)_3Cl$, and nano-Fe_3O_4@EA particles showed that ellagic acid was successfully connected to the nano-Fe_3O_4@EA@$Si(CH_2)_3Cl$ particles.

The XRD patterns of nano-Fe_3O_4@EA@$Si(CH_2)_3Cl$ and nano-Fe_3O_4@EA particles are presented in figure 4. The XRD analysis of the nano-Fe_3O_4@EA sample demonstrated that the diffraction peaks matched the expected pattern for nano-Fe_3O_4 [37]. The XRD pattern of the nano-Fe_3O_4@EA particles exhibited six peaks at 30.5 ^{O}, 35.8 ^{O}, 43.4 ^{O}, 53.6 ^{O}, 57.3 ^{O}, and 62.9 ^{O}, corresponding to the (220), (311), (400), (422), (511), and (440) reflection planes of Fe_3O_4 (JCPDS NO. 75-1609), respectively. These characteristic peaks were also observed in the XRD patterns of the nano-Fe_3O_4@EA, stating that the primary crystal phase structure of nano-Fe_3O_4@$Si(CH_2)_3Cl$ remained intact after ellagic acid conjugation.

The magnetic properties of nano-Fe_3O_4@$Si(CH_2)_3Cl$ and nano-Fe_3O_4@EA particles were investigated using VSM at 25 ^{O}C (see figure 5). The saturation magnetization of nano-

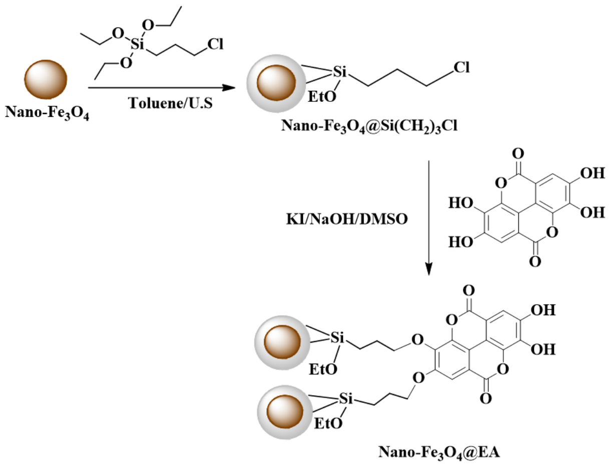

Figure 2. Schematic illustration of the nano-Fe_3O_4@EA.

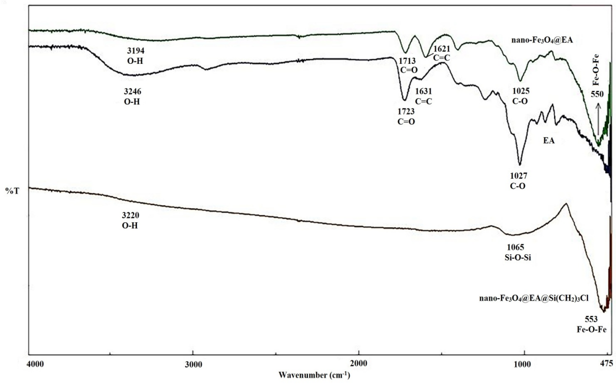

Figure 3. FT-IR spectra of: nano-Fe_3O_4@EA@$Si(CH_2)_3Cl$, ellagic acid (EA), and nano-Fe_3O_4@EA.

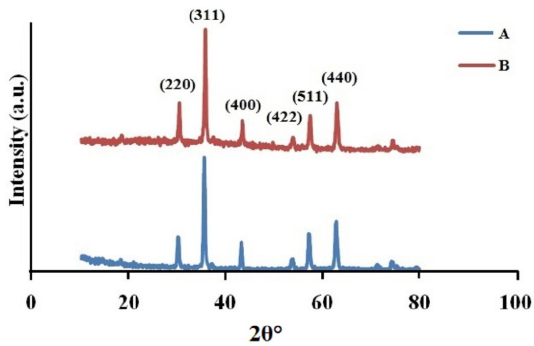

Figure 4. XRD diffraction patterns: A) nano-Fe_3O_4@$Si(CH_2)_3Cl$, and B) nano-Fe_3O_4@EA particles.

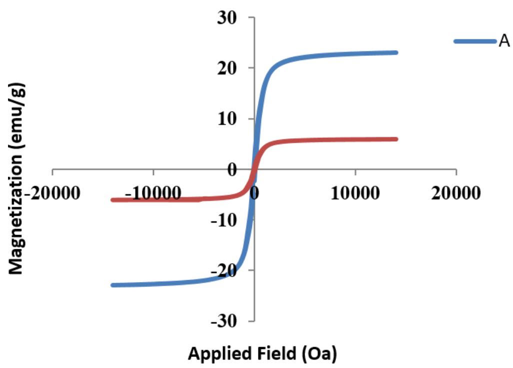

Figure 5. VSM image of nano-Fe_3O_4@$Si(CH_2)_3Cl$ (A) and nano-Fe_3O_4@EA (B)particles.

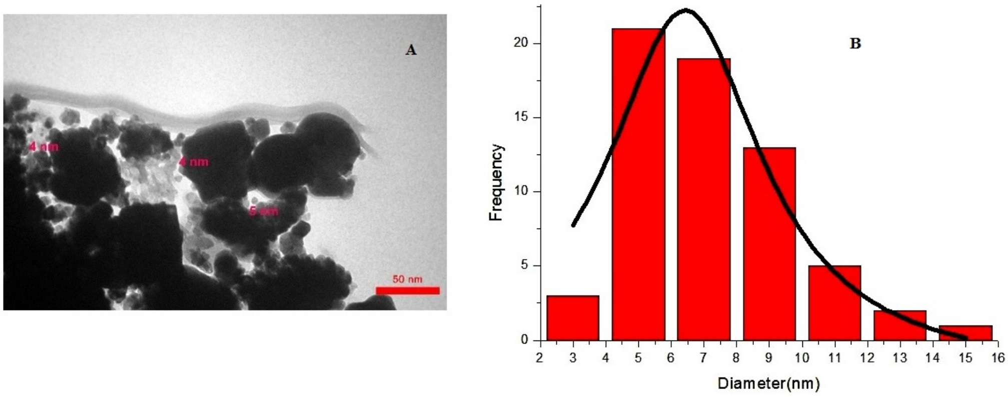

Figure 6. TEM image of nano-Fe_3O_4@EA (A) and histogram diagram of the nano-Fe_3O_4@EA (B).

Fe_3O_4@$Si(CH_2)_3Cl$ and nano-Fe_3O_4@EA particles was 22.5 emu g^{-1} and 5.9 emu g^{-1}, respectively. In comparison to nano-Fe_3O_4@$Si(CH_2)_3Cl$, the saturation magnetization of nano-Fe_3O_4@EA particles noticeably reduced due to the diamagnetic contribution of the thick SiO_2 and ellagic acid compounds.

The TEM micrograph of nano-Fe_3O_4@EA was characterized to examine its particle topology, distribution, and size. The TEM image of nano-Fe_3O_4@EA reveals a quasi-cube structure with minimal aggregation (figure 6 A). The histogram diagram of the nano-Fe_3O_4@EA (figure 6 B) shows particles ranging from approximately 5 to 8 nm with good dispersion.

3. Results and discussion

3.1 Investigating the effect of the solvent and temperature on the progress of the reaction

The reaction between ethyl-2-cyanoacetate and 4-formylphenylbenzenesulfonate was selected as the model reaction. Thin-layer chromatography was used to monitor the reaction. The impact of solvents on the synthesis of compound **3a** was examined by testing various solvents along with 0.05 g of nano-Fe_3O_4@EA catalyst. The findings are presented in Table 1. The research demonstrated that utilizing ethanol under reflux conditions yielded the most favorable outcomes.

The reaction between 1 mmol of ethyl cyanoacetate and 1 mmol of 4-formyl phenylbenzenesulfonate in ethanol, using 0.05 g of catalyst, was conducted at temperatures of 25 ^{o}C, 40 ^{o}C, and 78 ^{o}C. The results indicate that under reflux conditions (78 ^{o}C), product **3a** was obtained with the highest efficiency and in the shortest amount of time.

3.2 Effect of the catalyst amount in the reaction

To investigate the effect of the amount of nano-Fe_3O_4@EA catalyst, we conducted the model reaction using varying quantities of the catalyst (see Table 2). The results of our study indicate that employing 0.5 g of nano-Fe_3O_4@EA catalyst resulted in the production of **3a** product with optimal timing and efficiency.

This study demonstrated that in the presence of 0.05 g of nano-Fe_3O_4@EA as a catalyst in ethanol under reflux conditions, the desired products were efficiently formed in a timely manner. Therefore, all 2-cyano-3-phenylacrylate analogs considered in this study were prepared using the same conditions. The details of yield, reaction time, and their physical properties are reported in Table 3. To explore the scope of this reaction, various formylarylsulfonates were examined under the specified conditions (figure 7).

3.3 Proposed reaction mechanism

First, the nano-Fe_3O_4@EA catalyst activates the carbonyl aldehyde group through hydrogen bonding. Next, the methylene carbon of ethyl cyanoacetate forms intermediate **I** via a nucleophilic addition reaction. Finally, after removing water, the final product is synthesized (figure 8).

To assess the recyclability of the catalyst, it was utilized in the production of **3a** for five cycles under optimal con-

Table 1. Effects of various solvents on the preparation of compound 3a[a].

Entry	Solvent	Time (h)	Yield(%)[b]
1	MeCN	3	60
2	EtOAc	3	45
3	MeOH	3	70
4	-	3	35
5	EtOH	1	95

[a] Reaction conditions: 4-Formyl phenylbenzenesulfonate(1 mmol), ethyl cyanoacetate (1 mmol), and catalyst (0.05 g) in EtOH (5 mL) under reflux conditions.
[b] All yields refer to isolated products.

Table 2. Effect of the amount of the catalyst on the preparation of compound **3a**[a].

Entry	Amount of the catalyst (g)	Time (h)	Yield(%)[b]
1	-	4	30
2	0.01	3	48
3	0.03	2	72
4	0.05	2	95
5	0.06	2	95

[a] Reaction conditions: 4-Formyl phenylbenzenesulfonate(1 mmol), ethyl cyanoacetate (1 mmol), and catalyst(0.05 g) in EtOH (5 mL) under reflux conditions.
[b] All yields refer to isolated products.

Table 3. Synthesis of new ethyl cyanoacetate derivatives using nano-Fe_3O_4@EA catalyst[a].

Entry	Product	Time (h)	Yield(%)[b]	Mp (^{O}C)
3a	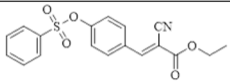	2	95	128-130
3b	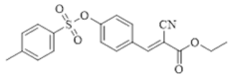	2.5	93	104-106
3c	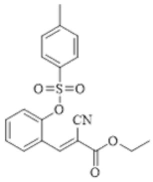	3	90	133-135
3d	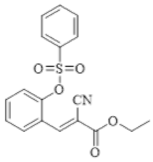	3	90	98-100
3e	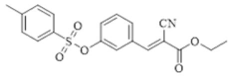	2	95	159-161
3f	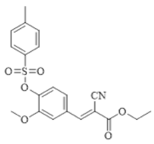	3	92	220-222
3g	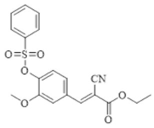	2.5	90	188-190
3h	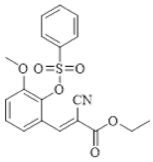	3	90	130-132
3i	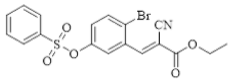	2	95	163-165

[a] Reaction conditions: Arylaldehyde (1 mmol), ethyl cyanoacetate(1 mmol), and catalyst(0.05 g) in EtOH (5 mL) under reflux conditions.
[b] All yields refer to isolated products.

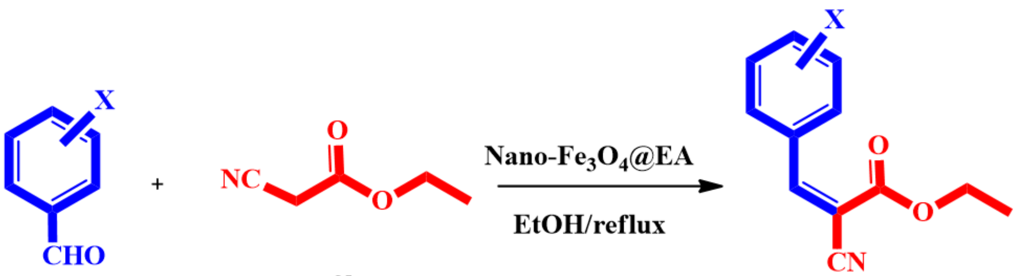

1(a-i) **2b** **3(a-i)**

Figure 7. Synthesis of new ethyl cyanoacetate analogs.

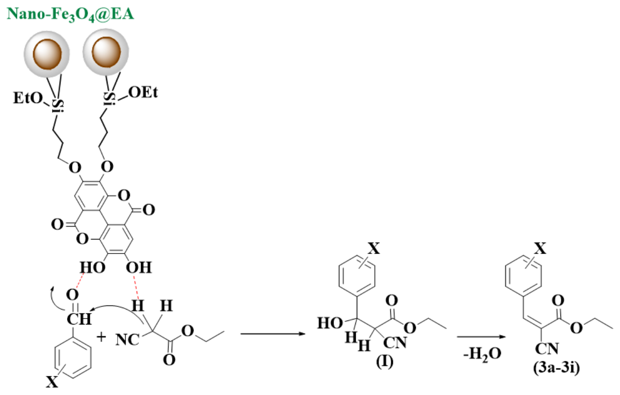

Figure 8. Proposed reaction mechanism.

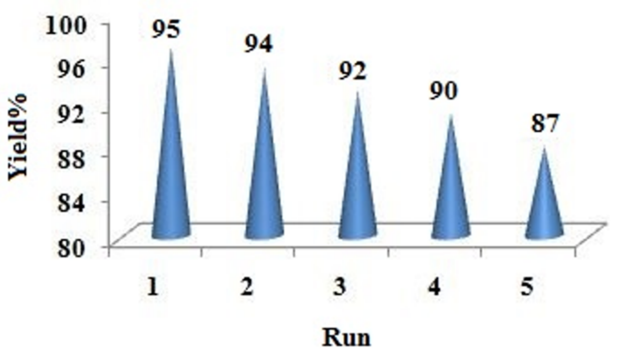

Figure 9. Reusability of nano-Fe_3O_4@EA in the synthesis of product **3a**.

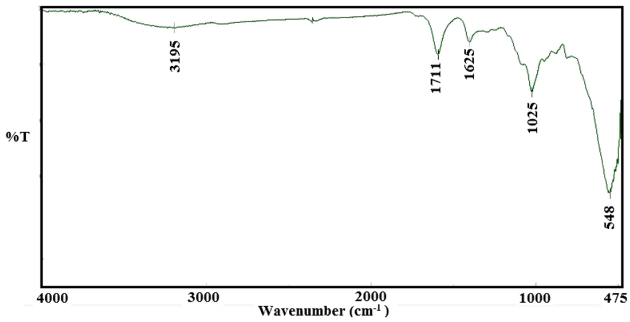

Figure 10. FT-IR spectra of nano-Fe_3O_4@EA after 5 runs.

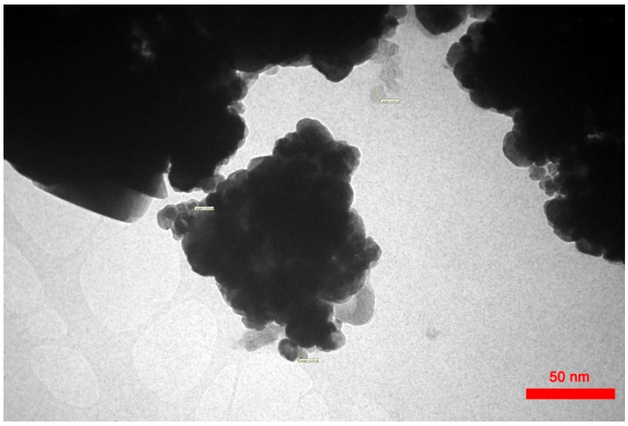

Figure 11. TEM image of nano-Fe_3O_4@EA after 5 runs.

ditions. It was then reused through magnetic isolation and washed with CH_2Cl_2. Following this, the required amount of fresh 4-formyl phenylbenzenesulfonate (1 mmol) and ethyl-cyanoacetate (1 mmol) were added based on the catalyst quantity. The findings indicated that the nano-Fe_3O_4@EA catalyst can be reused up to five times without a significant decrease in its catalytic efficiency (figure 9). The stability of the catalyst was explored through FT-IR and TEM analysis. The FT-IR spectrum of the reused catalyst is shown in Fig. 10, indicating no change after 5 uses. Additionally, SEM analysis results revealed that the morphology of the catalyst remained unchanged after 5 reuses (Fig. 11).

4. Conclusion

This research presents an effective method for synthesizing new derivatives of Knoevenagel ethyl cyanoacetate using nano-Fe_3O_4@EA as a magnetic catalyst. The unique characteristics of nano-Fe_3O_4@EA catalyst, such as high yield and simplicity of the process, make this method an attractive option for synthesizing Knoevenagel ethyl cyanoacetate. In this study, compounds of 2-cyano-3-phenyl acrylates were successfully synthesized. The use of nano-Fe_3O_4@EA as a catalyst yielded very favorable results due to its nanoparticle structure and the ability to adjust its functional groups.The attractive features of this work include easy process work-up, mild reaction conditions, absence of by-products, and the reusability of the nanocatalyst. The method presented is highly suitable for the synthesis of Knoevenagel adducts with high yields.

Acknowledgment

Financial support of Islamic Azad University, Rasht branch is appreciated.

Authors contributions

Authors have contributed equally in preparing and writing the manuscript.

Availability of data and materials

The authors declare that the data supporting the findings of this study are available from corresponding author upon reasonable requaest.

Conflict of interests

The authors declare no conflict of interest.

References

[1] F. Freeman. "Properties and reactions of ylidenemalononitriles.". *Chem. Rev.*, 80:329–350, 1980. DOI: https://doi.org/10.1021/cr60326a004.

[2] G. A. Kraus and M. E. Krolski. "Synthesis of a precursor to quassimarin.". *J. Org. Chem.*, 51:3347–3350, 1986. DOI: https://doi.org/10.1021/jo00367a017.

[3] L. F. Tietze and N. Rackelmann. "Domino reactions in the synthesis of heterocyclic natural products and analogs.". *Pure Appl. Chem.*, 76:1967–1983, 2004. DOI: https://doi.org/10.1351/pac200476111967.

[4] S. Knezevic, A. Ghafoor, S. Mehri, A. Barazi, M. Dziura, J. F. Trant, and C. A. Dieni. "Catechin and other catechol-containing secondary metabolites: Bacterial biotransformation and regulation of carbohydrate metabolism.". *PharmaNutrition*, 17:100273, 2021. DOI: https://doi.org/10.1016/j.phanu.2021.100273.

[5] E. C. Rietveld, M. A. Garnaat, and F. Seutter-Berlage. “Bacterial mutagenicity of some methyl 2-cyanoacrylates and methyl 2-cyano-3-phenylacrylates.”. *Mutat. Res.*, 188:97–104, 1987. DOI: https://doi.org/10.1016/0165-1218(87)90097-8.

[6] E. C. Rietveld, W. J. M. Engels, R. Smit, and F. Seutter-Berlage. “Metabolism of some methyl 2-cyano-3-phenyl-acrylates (methyl α-cyanocinnamates) in Rats.”. *Xenobiotica*, 19:477–488, 1989. DOI: https://doi.org/10.3109/00498258909042287.

[7] H. Teichmann and W. Thierfelder. “Phosphous function addition to substituted olefins.”. *Ger Patent (East)*, 129, 1978.

[8] H. Oba, T. Murayama, and S. Otsuka. “Photosensitive composition for electro-photography.”. *US patent*, 4(184):871, 1998.

[9] A. T. Peters, M. S. Wild, and S. J. Otsuka. “”. *Soc. Dyes Colour*, 93: 347, 1994.

[10] E. M. Schneider, M. Zeltner, N. Kranzlin, R. N. Grass, and W. J. Stark. “Base-free Knoevenagel condensation catalyzed by copper metal surfaces.”. *Chem. Commun.*, 51:10695, 2015. DOI: https://doi.org/10.1039/C5CC02541A.

[11] M. Venkatanarayana and P. K. Dubey. “L-Proline-catalyzed Knoevenagelcondensation: afacile, green synthesis of (E)-ethyl 2-cyano-3-(1H-indol-3-yl)acrylates and (E)-3-(1H-indol-3-yl)acrylonitriles.”. *Synth. Commun.*, 42:1746–1759, 2012.

[12] R. Kada, D. Ilavsky, J. Stetinova, L. Zalibera, and J. Padour. “Synthesis, reactions and spectral properties of ethyl esters of 2-cyano-3-(5-X-2-furyl)acrylic acid, Collect.”. *Czechoslov. Chem. Commun.*, 59:444–452, 1994. DOI: https://doi.org/10.1135/cccc19940444.

[13] B. Xu, Z. Liu, Q. Xu, X. Han, X. Ma, J. Wang, T. Kannan, P. Ma, J. Wang, and J. Niu. “Polyoxomolybdates as efficient catalysts for Knoevenagel condensation reaction of benzaldehyde and ethyl cyanoacetate under mild condition.”. *J. Mater. Sci.*, 56:4654–4665, 2021. DOI: https://doi.org/10.1007/s10853-020-05562-x.

[14] K. A. Almeida and D. Cardoso. “Basic activity of Y zeolite containing alkylammonium cations in Knoevenagel condensation.”. *Catal. Today*, 213:122–126, 2013. DOI: https://doi.org/10.1016/J.CATTOD.2013.03.011.

[15] F. Hajizadeh, B. Maleki, F. MohammadiZonoz, and A. Amiri. “Application of structurally enhanced magnetite cored polyamidoamine dendrimer for Knoevenagel condensation.”. *J. Iran. Chem. Soc.*, 18: 793–804, 2021. DOI: https://doi.org/10.1007/s13738-020-02071-1.

[16] S. Arbabi Jam, Y. Sarrafi, and B. Maleki. “Immobilization of ionic liquid–triethanolammonium bicarbonate on magnetic nanoparticles as an efficient catalyst for knovenegel condensation.”. *Polycyclic Aromat. Compd.*, 44:4364–4375, 2024. DOI: https://doi.org/10.1080/10406638.2023.2247129.

[17] S. Falah, M. Soleiman-Beigi, and H. Kohzadi. “Potassium Natural Asphalt Sulfonate (K- NAS): Synthesis and characterization as a new recyclable solid basic nanocatalyst and its application in the formation of carbon–carbon bonds.”. *ApplOrganomet. Chem.*, 34: e5840, 2020. DOI: https://doi.org/10.1002/aoc.5840.

[18] F. Ghobakhloo, D. Azarifar, M. Mohammadi, H. Keypour, and H. Zeynali. “Copper(II) schiff-base complex modified UiO-66-NH2(Zr) metal-organic framework catalysts for Knoevenagel condensation-Michael addition-cyclization reactions.”. *Inorg.Chem.*, 61:4825–4841, 2022. DOI: https://doi.org/10.1021/acs.inorgchem.1c03284.

[19] S. Nosratollahi, M. Soleiman-Beigi, and M. Norouzi. “ A chemoselective and one-pot method for the synthesis of unsymmetrical secondary amines via coupling reaction ofammonia and aryl(alkyl) halides catalyzed by MNP@IAH@Cu-IL as a bifunctional nanocatalyst.”. *Appl. Organomet. Chem.*, 38:e7462, 2024. DOI: https://doi.org/10.1002/aoc.7462.

[20] M. Borzooei, M. Norouzi, and M. Mohammadi. “Construction of a dual-functionalized acid-base nanocatalyst via HEPES buffer functionalized on Fe_3O_4 as a reusable catalyst for annulation reactions.”.

[21] H. Kohzadi and M. Soleiman-Beigi. “XPS and structural studies of Fe_3O_4-PTMS-NAS@Cu as a novel magnetic natural asphalt base network and recoverable nanocatalyst for the synthesis of biaryl compounds.”. *Sci. Rep.*, 11:24508, 2021. DOI: https://doi.org/10.1038/s41598-021-04111-z.

[22] A. Nikseresht, M. Karami, and M. Mohammadi. “Phosphotungsticacid-supported Hercynite: amagnetic nanocomposite catalyst for the selective esterification of chloroaceticacid.”. *Langmuir*, 40(35):18512–18524, 2024. DOI: https://doi.org/10.1021/acs.langmuir.4c01763.

[23] M. Mokhtary. “Recent advances in catalysts immobilized on magnetic nanoparticles.”. *J. Iran. Chem. Soc.*, 13:1827–1845, 2016. URL https://link.springer.com/article/10.1007/s13738-016-0900-4.

[24] M. Mokhtary and M. Torabi. “Nano magnetite (Fe_3O_4), an efficient and robust catalyst for the one-pot synthesis of 1-(aryl(piperidin-1-yl)methyl)naphthalene-2-ol and 1-(α-amido alkyl)-2-naphthol under ultrasound irradiation.”. *J. Saudi Chem. Soc.*, 21:S299–S304, 2017. DOI: https://doi.org/10.1016/j.jscs.2014.03.009.

[25] A. Gholami, M. Mokhtary, and M. Nikpassand. “Glycolic acid-supported cobalt ferrite-catalyzed one-pot synthesis of pyrimido[4,5-b]quinoline and indenopyrido[2,3-d]pyrimidine derivatives.”. *Appl. Organomet. Chem.*, 34:e6007, 2020. DOI: https://doi.org/10.1002/aoc.6007.

[26] F. Haghighat and M. Mokhtary. “Preparation and characterization of polyvinylpyrrolidone/Magnetite decorated carboxylic acid functionalized multi-walled carbon nanotube (PVP/MWCNT-Fe_3O_4) nanocomposite.”. *J. Inorg. Organomet. Polym. Mater.*, 27:779–787, 2017. URL https://link.springer.com/article/10.1007/s10904-017-0521-0.

[27] M. ForoughiKaldareh, M. Mokhtary, and M. Nikpassand. “Nicotinic acid-supported cobalt ferrite-catalyzed one-pot synthesis of substituted chromeno[3,4-b]quinolines.”. *Appl. Organomet. Chem.*, 34: e5469, 2020. DOI: https://doi.org/10.1002/aoc.5469.

[28] M. Masoumparast, M. Mokhtary, and H. Kefayati. “Preparation and characterization of polyvinylpyrrolidone/cobalt ferrite functionalized chitosan graphene oxide ($CoFe_2O_4$@CS@GO-PVP) nanocomposite.”. *J. Polym. Eng.*, 40:342–349, 2020. DOI: https://doi.org/10.1515/polyeng-2019-0331.

[29] S. Ghiassi, M. Mokhtary, S. Sedaghat, and H. Kefayati. “Preparation, and antibacterial activity of chloroacetic acid immobilized on chitosan coated iron oxide decorated silver nanoparticles as an efficient catalyst for the systhesis of Hexahydroquinoline-3-Carboxamides.”. *J. Inorg. Organomet. Polym. Mater.*, 29:1972–1982, 2019. URL https://link.springer.com/article/10.1007/s10904-019-01156-6.

[30] B. Babaei, M. Mamaghani, and M. Mokhtary. “Sustainable approach to the synthesis of 1,4-disubstitued triazoles using reusable Cu(II) complex supported on hydroxyapatite-encapsulated α-Fe_2O_3 as organic–inorganic hybrid nanocatalyst.”. *React. Kinet. Mech. Catal.*, 128:379–394, 2019. URL https://link.springer.com/article/10.1007/s11144-019-01636-3.

[31] B. Babaei, M. Mamaghani, and M. Mokhtary. “Clean synthesis of propargylamines using novel magnetically recyclable silver nanocatalyst (AgMNPs).”. *Polycycl, Aromat. Compd.*, 43:396–408, 2023. URL https://www.tandfonline.com/doi/full/10.1080/10406638.2021.2015401.

[32] A. Gholami, M. Mokhtary, S. SetarehAttarseyedi, B. Masoumi, and M. Mamaghani. “Synthesis of polyfunctionalized furan analogs catalyzed by chlorosulfonic acid immobilized nano-Cobaltferrite.”. *J. Clust. Sci.*, 35:69–78, 2024. URL https://link.springer.com/article/10.1007/s10876-023-02462-3.

[33] D. Collado, E. Perez-Inestrosa, R. Suau, and J. T. Lopez Navarrete. "Regioselective hydroxylation of phenols by simultaneous photochemical generation of phenol cation-radical and hydroxyl radical.". *Tetrahedron*, 62:2927–2935, 2006. DOI: https://doi.org/10.1016/j.tet.2006.01.003.

[34] K. Freudenberg and H. Hess. "Ein verfahrenzur kennzeichnungverschiedenartiger Hydroxylgruppen.Seine Anwendung auf das Lignin.". *Justus LiebigsAnnalen der Chemie*, 448:121–133, 1962. DOI: https://doi.org/10.1002/jlac.19264480110.

[35] F. M. Piller, A. Metzger, M. A. Schade, B. A. Haag, A. Gavryushin, and P. Knochel. "Preparation of polyfunctionalarylmagnesium, arylzinc, and benzylic zinc reagents by using magnesium in the presence of LiCl.". *Chem.–A Eur. J.*, 15:192–7202, 2009. URL https://chemistry-europe.onlinelibrary.wiley.com/doi/10.1002/chem.200900575.

[36] C. Nadler, A. Nadler, C. Hansen, and U. Diederichsen. "Aphotocleavable auxiliary for extended native chemical ligation.". *Eur. J. Org. Chem.*, pages 3095–3102, 2015. URL https://chemistry-europe.onlinelibrary.wiley.com/doi/abs/10.1002/ejoc.201500033.

[37] N. Azgomi and M. Mokhtary. "Nano-Fe_3O_4@SiO_2 supported ionic liquid as an efficient catalyst forthe synthesis of 1,3-thiazolidin-4-ones under solvent-free conditions.". *J. Mol. Catal. A: Chem.*, 398: 58–64, 2015. DOI: https://doi.org/10.1016/j.molcata.2014.11.018.